Mechanism of Formation and Growth of ⟨100⟩ Interstitial Loops in Ferritic Materials

Jaime Marian* and Brian D. Wirth

Chemistry and Materials Science Directorate, Lawrence Livermore National Laboratory, P.O. Box 808, L-353, Livermore, California 94550

J. Manuel Perlado

Instituto de Fusión Nuclear, Universidad Politécnica de Madrid, C/ José Gutiérrez Abascal, 2, Madrid 28006, Spain

(Received 18 December 2001; published 11 June 2002)

We propose a comprehensive mechanism for the formation and growth of ⟨100⟩ interstitial loops in α-Fe. This mechanism reconciles long-standing experimental observations of these defects in irradiated ferritic materials with recent atomistic simulations of collision cascades and defect cluster properties in Fe, in which highly mobile $\frac{1}{2}\langle 111\rangle$ clusters are seen to be the dominant feature. Hence, this work provides one of the necessary links to unify simulation with experiments in α-Fe and ferritic alloys subject to high-energy particle irradiation.

DOI: 10.1103/PhysRevLett.88.255507 PACS numbers: 61.72.Bb, 61.72.Ji, 61.80.Az, 61.82.Bg

Ferritic steels and alloys represent a technologically important class of materials that are widely used for structural purposes in current nuclear fission reactors and proposed as candidate materials for plasma-facing first wall structures in future fusion energy facilities. Predicting their in-service performance requires understanding the accumulation of defects and evolution of the microstructure under the severe irradiation conditions found in these environments.

It is well established that examination of ferritic alloys by transmission electron microscopy (TEM) following low dose irradiation ($\lesssim$0.1 displacement per atom, dpa) by neutrons or heavy ions does not reveal any visible damage. However, as the irradiation dose increases above $\sim$1 dpa, a significant population of prismatic dislocation loops, presumably of interstitial type, is experimentally observed. In contrast to other bcc alloys, such as Mo and V, the dislocation loops have Burgers vectors, $b = \langle 100\rangle$ and $b = \frac{1}{2}\langle 111\rangle$ in almost equal proportions, rather than predominantly $\frac{1}{2}\langle 111\rangle$. While this result has been known for nearly 40 years [1–6], the mechanisms responsible for the presence of ⟨100⟩ loops in ferritic alloys are not yet well understood.

A comparison of the dislocation loop energy based on continuum elasticity estimates (elastic energy proportional to Gb^2, where G is the shear modulus) indicates that $\frac{1}{2}\langle 111\rangle$ loops are energetically favored and, thus, the observation of ⟨100⟩ loops in α-Fe and other ferritic alloys has remained a puzzle. In 1965, Eyre and Bullough [7] proposed a mechanism by which ⟨100⟩, as well as $\frac{1}{2}\langle 111\rangle$, dislocation loops could form from an aggregate of $\frac{1}{2}\langle 110\rangle$ self-interstitials through shear reactions of the type

$$\tfrac{1}{2}[110] + \tfrac{1}{2}[00\bar{1}] \rightarrow \tfrac{1}{2}[11\bar{1}], \quad (1)$$

$$\tfrac{1}{2}[110] + \tfrac{1}{2}[\bar{1}10] \rightarrow [010]. \quad (2)$$

Again, consideration of the dislocation energy of the two reactions reveals a puzzle as to why ⟨100⟩ loops would form rather than $\frac{1}{2}\langle 111\rangle$. Additionally, the Eyre and Bullough mechanism is predicated on the formation of platelets of self-interstitial atoms (SIA) with Burgers vector $b = \frac{1}{2}\langle 110\rangle$, which corresponds to a faulted dislocation loop. However, the high stacking fault energy of bcc materials discounts the formation and stability of faulted loops and, thus, one can safely conclude that the Eyre and Bullough mechanism is not plausible to describe the formation of ⟨100⟩ interstitial loops in ferritic alloys.

Indeed, recent molecular dynamics (MD) simulations of self-interstitial cluster geometry using Finnis-Sinclair, embedded atom-type, and long-range pair potentials reveal that stable interstitial cluster configurations for sizes from $n \geq 2$ consist of aggregates of $\frac{1}{2}\langle 111\rangle$-oriented, rather than $\frac{1}{2}\langle 110\rangle$, split dumbbells [8–10]. Clusters of $\frac{1}{2}\langle 111\rangle$ self-interstitials have very high mobility for one-dimensional (1D) motion along ⟨111⟩ directions up to very large sizes ($n \gtrsim 100$). As well, MD simulations of displacement cascade evolution have consistently revealed the formation of SIA clusters with ⟨111⟩ orientations, which again exhibit high mobility [11,12]. In this Letter we provide a mechanism for the formation and growth of ⟨100⟩ dislocation loops that reconciles the long-standing experimental observation of these defects in irradiated ferritic materials with recent MD studies of $\frac{1}{2}\langle 111\rangle$ cluster stability, their production in displacement cascades, and high mobility in one dimension. We first describe in detail the energetics of $\frac{1}{2}\langle 111\rangle$ and ⟨100⟩ interstitial dislocation loops, then propose a mechanism for ⟨100⟩-loop nucleation, which involves the direct interaction of migrating $\frac{1}{2}\langle 111\rangle$ loops, and, finally, a growth mechanism for ⟨100⟩ loops to reach TEM visible sizes.

Clearly, an energetics analysis based exclusively on isotropic, continuum elastic energy considerations (Gb^2) is insufficient to describe the loop interaction dynamics, as it ignores important contributions such as loop shape, angle between the habit plane and the Burgers vector, and

anisotropy effects. An analysis of the energetics of $\frac{1}{2}\langle 111\rangle$ and $\langle 100\rangle$ loops that takes into account all such contributions is attained by way of fully atomistic, MD relaxations at low temperatures, followed by a conjugate-gradient energy minimization to obtain the configuration-dependent loop energies. The configurations of interest for $b = \langle 100\rangle$ loops are those with $\{110\}$ and $\{100\}$ habit planes (corresponding to the closest-packed and perfect edge configurations). In terms of loop shape, the minimum-energy configurations correspond to loop sides oriented along the close-packed directions in each habit plane, i.e., rhombic $\langle 100\rangle\{110\}$ loops and square or rectangular $\langle 100\rangle\{100\}$ loops (the most stable configuration for $\frac{1}{2}\langle 111\rangle$ loops has been reported to be hexagonal-shaped $\frac{1}{2}\langle 111\rangle\{110\}$ [9,10]). All atomistic results have been obtained with the MDCASK code [13] in which the Finnis-Sinclair–type potentials for Fe derived by Ackland *et al.* [14] have been implemented.

Figure 1 presents the three corresponding formation energy curves, obtained through a nonlinear fit to the MD data (also shown) using the continuum elasticity expression for the self-energy, E_l, of a prismatic dislocation loop as given by Hirth and Lothe [15]:

$$E_l = \frac{NL\mu b^2}{4\pi(1-\nu)}\left[\ln\left(\frac{L}{\rho}\right) + C\right]. \tag{3}$$

Here N is the number of sides of the loop, L is the side length, μ and ν the shear modulus and Poisson's ratio, b is the Burger's vector magnitude, and ρ and C represent the dislocation core cutoff radius and a constant that includes the dislocation core energy. Using the elastic constant values calculated from the α-Fe potential used here and values of $\rho = b/4$ and $\rho = b$ for the cutoff radii of $\frac{1}{2}\langle 111\rangle$ and $\langle 100\rangle$ loops, we obtain core energies of 0.38 and 1.10 eV/Å, respectively. The value for $\frac{1}{2}\langle 111\rangle$ loops is consistent with results reported in the literature [9,16], while, to our knowledge, the core energy value for the

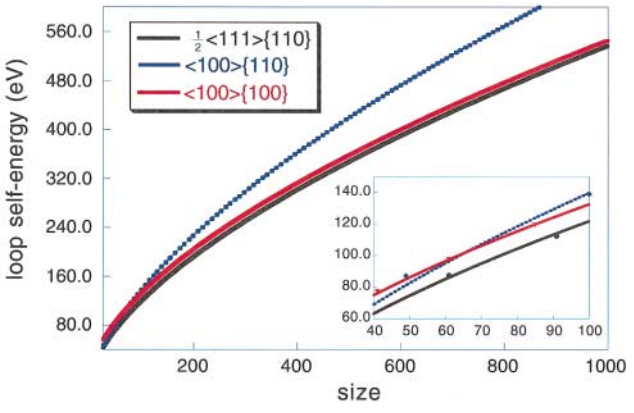

FIG. 1 (color). Dislocation loop energy as a function of size (number of constituent interstitials). The curves result from fits of Eq. (3) to the MD data points. The inset showcases the energies at smaller sizes, where the crossing of the energies of $\langle 100\rangle\{110\}$ and $\langle 100\rangle\{100\}$ loops is emphasized.

$\langle 100\rangle$ dislocation loops represents the first calculation reported to date. The high value for both the dislocation loop core radii and core energy for $\langle 100\rangle$ loops suggests the existence of large tensile forces around the core region of the loop, which diminishes the validity of a purely isotropic elastic analysis.

As seen in Fig. 1, $\frac{1}{2}\langle 111\rangle$ loops are the most stable configurations, consistent with previous continuum elasticity estimates, although the energy difference between $\frac{1}{2}\langle 111\rangle$ and $\langle 100\rangle\{100\}$ configurations becomes very small ($<10\%$) for larger loop sizes. Initially, $\langle 100\rangle$ loops are more stable on $\{110\}$ habit planes but, with increasing size, $\langle 100\rangle\{100\}$ configurations become energetically favored, with a crossing around $n \sim 68$. Presumably, this results from the reduction in dislocation segment length for $\langle 100\rangle$ loops on $\{100\}$ rather than $\{110\}$ habit planes.

It has long been recognized that reactions between dislocations with Burgers vectors $b = \frac{1}{2}\langle 111\rangle$ can occur according to

$$\tfrac{1}{2}[111] + \tfrac{1}{2}[1\bar{1}\bar{1}] \rightarrow [100]. \tag{4}$$

This can lead to the formation of $\langle 100\rangle$ junctions and dislocation segments, which have been mainly observed in dislocation networks in Fe [17,18]. As well, such reactions between $\frac{1}{2}\langle 111\rangle$-type loops can give rise to the formation of $\langle 100\rangle$ loops. Indeed, Masters proposed such a mechanism in 1965 [1], yet discounted it due to a lack of observed loops with $b = \frac{1}{2}\langle 111\rangle$ in thin-film ion irradiation studies.

In order to shed light onto the formation of $\langle 100\rangle$ loops, we have performed extensive MD simulations of interactions between $\frac{1}{2}\langle 111\rangle$ loops. One such interaction consisted of hexagonal and jogged hexagonal $\frac{1}{2}\langle 111\rangle$ loops with $n = 37$ and 34, respectively, with intersecting glide prisms, akin to Eq. (4). Figure 2 shows a sequence of snapshots from the MD simulation at 1000 K. The two loops glide towards one another and collide, driven by the energy reduction that results when two loops condense into a single loop containing the same total number of interstitials. A $[100]$ junction consisting of five SIAs on a (110) plane formed instantaneously following the collision [Fig. 2(b)]. A similar phenomenon has been reported in Fe by Osetsky *et al.* [19].

The peculiarity of this interaction is that the glide direction of each loop is contained in the habit plane of the other interacting loop, and thus, once the loops collide, the dislocation segments of Burgers vector $\frac{1}{2}[111]$ can continue to glide within the loop of Burgers vector $\frac{1}{2}[1\bar{1}\bar{1}]$. By reaction 4, this produces dislocation segments with Burgers vector $[100]$ on both sides of the contact point. Given enough time, both $\frac{1}{2}\langle 111\rangle$ loops will gradually transform into a single entity with Burgers vector $b = \langle 100\rangle$. Therefore, we propose that $\langle 100\rangle$ loops initially form as $\langle 100\rangle$ junctions on $\{110\}$ planes in collisions between $\frac{1}{2}\langle 111\rangle$ loops and grow outward until the defect boundaries are reached. As the $\langle 100\rangle$ segments grow and the elastic

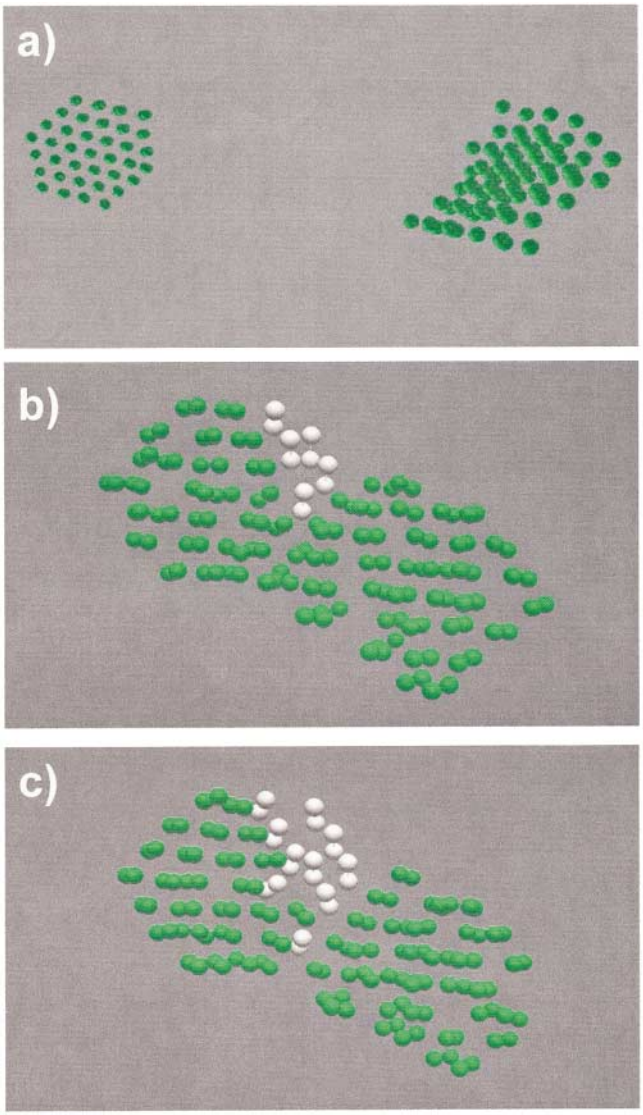

FIG. 2 (color). Sequence of MD snapshots at (a) 0, (b) 120, and (c) 430 ps, of the interaction of two $\frac{1}{2}\langle 111\rangle$ loops with Burgers vectors appropriate to Eq. (4) (see text).

energy density (stress) builds up, the cluster will eventually rotate onto {100} habit planes. A large number of cluster-interaction simulations involving different cluster shapes and sizes have been performed, and, in all cases, the main observation is that the intersecting loops need to be of approximately the same size, and possibly shape, to stabilize and grow $\langle 100\rangle$-type segments. When these constraints are not met, the smaller cluster always rotates into the $\frac{1}{2}\langle 111\rangle$ orientation of the larger cluster.

The high energies associated with having multiple dislocation segments within a loop make the propagation of the $\langle 100\rangle$ segments a complex process at the atomic scale, since $\frac{1}{2}\langle 111\rangle$ dislocation segments no longer glide through perfect, close-packed directions but, instead, through a plane containing oppositely oriented interstitials. Visualization of the MD simulations revealed that the $\langle 100\rangle$ segments (best thought of as an array of akin self-interstitial atoms) propagate throughout the loop according to the following two-step reaction:

$$\tfrac{1}{2}[111] + \tfrac{1}{2}[00\bar{1}] \rightarrow \tfrac{1}{2}[110], \quad (5)$$

$$\tfrac{1}{2}[110] + \tfrac{1}{2}[1\bar{1}0] \rightarrow [100]. \quad (6)$$

Thus, the interstitials reach their final [100] orientation by way of a modified Eyre-Bullough mechanism (modified reaction 1 and direct reaction 2). This is a thermally activated process by which SIAs at the $\frac{1}{2}\langle 111\rangle$-$\langle 100\rangle$ nodes, e.g., with $\frac{1}{2}[111]$ orientation, first undergo a partial $[00\bar{1}]$ shear into a metastable $\frac{1}{2}[110]$ configuration with an activation energy of $\sim$0.5 eV. This produces large repulsive interactions with adjacent [100] dumbbells that force the metastable $\frac{1}{2}[110]$ dumbbell to further rotate into a more favorable configuration. This can be attained by the $\frac{1}{2}[110]$ dumbbell reversing its original trajectory back to the $\frac{1}{2}[111]$ orientation, or rotating into a [100] orientation through reaction 6, with an activation barrier of the order of 1.0 eV.

The nearly immediate formation of the $\langle 100\rangle$ nucleus upon cluster collision is a consequence of the interaction process governed by Eq. (4) and driven by the energy reduction associated with forming a single cluster. The growth vs shrinkage of the $\langle 100\rangle$ junctions (loops) [Eqs. (5) and (6)] is governed by the interaction energy landscape, schematically shown in Fig. 3. The rate at which [100] growth is sampled ($\langle 111\rangle$ to $\langle 110\rangle$ to $\langle 100\rangle$) is favored with respect to its dissolution (inverse path), which, integrated over sufficiently long times, results in an effective $\langle 100\rangle$-loop transformation. For example, after 300 ps [Fig. 2(c)] five additional interstitials forming part of the $\frac{1}{2}[1\bar{1}\bar{1}]$ (left) loop rotated into a [100] orientation and resided in that configuration during the entire simulation (1 ns). The direct rotation from a $\langle 111\rangle$ to

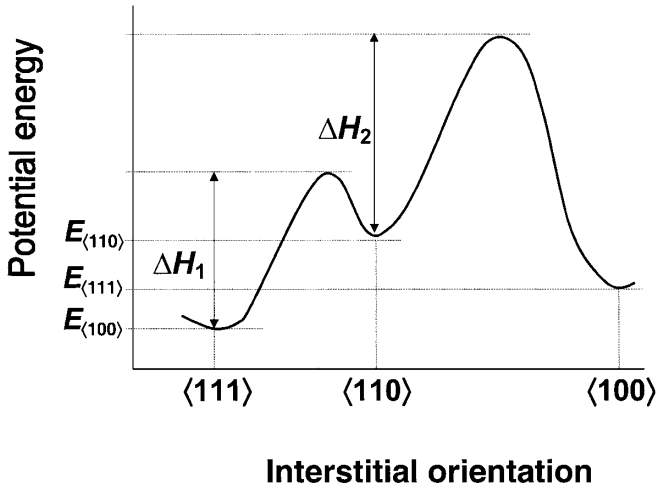

FIG. 3. Schematic illustration of the reaction energy landscape, for the propagation and transformation of $\frac{1}{2}\langle 111\rangle$ dislocation segments into $\langle 100\rangle$ segments within the interacting $\frac{1}{2}\langle 111\rangle$ loops. Depending on loop size and shape, ΔH_1 and ΔH_2 are of the order of 0.5 and 1.0 eV, respectively.

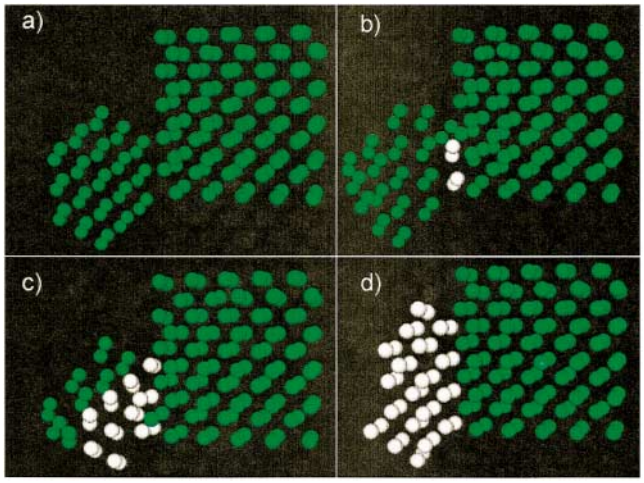

FIG. 4 (color). Sequence of MD snapshots at (a) 0.0, (b) 1.5, (c) 2.2, and (d) 3.5 ps, of the absorption of one hexagonal, 19-SIA $\frac{1}{2}[111](110)$ cluster by a square, 50-SIA $[100](100)$ loop according to Eq. (7) at 100 K. Interstitials displayed in white are those belonging to the $\frac{1}{2}[111]$ cluster that have rotated to a $[100]$ configuration.

a $\langle 100\rangle$ orientation, or vice versa, can be neglected, since it requires energies in excess of 2.0 eV. This provides an explanation as to why, at moderate temperatures, the final configuration resulting from the interaction of two $\frac{1}{2}\langle 111\rangle$ loops consists of metastable $\langle 100\rangle$ loops, rather than the slightly lower-energy $\frac{1}{2}\langle 111\rangle$ loops.

The remaining point to consider is how $\langle 100\rangle$ clusters grow to TEM observable sizes. Although intrinsically glissile owing to their pure-edge prismatic nature, the crystal structure dictates that $\langle 100\rangle\{100\}$ loops require a large jump distance. This results in a very high activation energy, computed to be >2.5 eV. Thus, once formed, $\langle 100\rangle$ loops are essentially stationary and can act as biased sinks for mobile, cascade-produced $\frac{1}{2}\langle 111\rangle$ loops. Notably, MD simulations of interactions between $\frac{1}{2}\langle 111\rangle\{110\}$ and $\langle 100\rangle\{100\}$ loops reveal $\langle 100\rangle$ loop growth. Figure 4 shows one such interaction in which a 19-SIA $\frac{1}{2}\langle 111\rangle$ cluster is absorbed by a 50-SIA $\langle 100\rangle$ square loop. Even though the lowest energy configuration corresponds to a 69-SIA $\frac{1}{2}\langle 111\rangle$ loop, the system follows the path of least resistance into a 69-SIA $\langle 100\rangle$ loop through the following atomic-level reaction:

$$\langle 100\rangle + 2(\tfrac{1}{2}\langle 111\rangle) \rightarrow \langle 211\rangle \rightarrow \langle 100\rangle, \qquad (7)$$

i.e., rotation of individual $\langle 111\rangle$-oriented interstitials in the presence of $\langle 100\rangle$ SIAs into an intermediate metastable $\langle 211\rangle$ configuration that rapidly rotates into a $\langle 100\rangle$ orientation.

In summary, based on extensive MD simulations of $\frac{1}{2}\langle 111\rangle$-$\frac{1}{2}\langle 111\rangle$ and $\langle 100\rangle$-$\frac{1}{2}\langle 111\rangle$ interactions, we propose a comprehensive mechanism for the nucleation and growth of TEM visible $\langle 100\rangle$ loops. This mechanism is consistent with both experimental observations and with the current understanding of interstitial cluster formation, diffusion, and growth from atomistic simulations. SIAs produced in collision cascades initially aggregate as small $\frac{1}{2}\langle 111\rangle$ clusters. These clusters either rapidly migrate to system sinks or interact with each other. The $\langle 100\rangle$ nuclei form through the direct interaction of $\frac{1}{2}\langle 111\rangle$ clusters of comparable size via Eq. (4). The two interacting dislocation loops propagate through each other's habit plane according to reactions (5) and (6), resulting in the ultimate growth of the $\langle 100\rangle\{110\}$ junction until the whole loop is transformed. The resulting loops are metastable with respect to $\frac{1}{2}\langle 111\rangle$, but the energy differences can be quite small and the activation barrier to reorient into $\langle 111\rangle$ orientations quite large. With increasing size, $n > 68$, $\langle 100\rangle\{110\}$ loops rearrange onto $\{100\}$ habit planes. In this configuration, $\langle 100\rangle$ loops are metastable and practically immobile, allowing for the absorption of other small $\frac{1}{2}\langle 111\rangle$ clusters via a direct-rotation mechanism (reaction 7) that allows $\langle 100\rangle$-loop growth up to TEM observable sizes.

This work has been performed under the auspices of the U.S. Department of Energy and Lawrence Livermore National Laboratory under Contract No. W-7405-Eng-48 and within the CSN-UNESA Coordinated Research Programme under Contract No. P000531499.

*Email address: marian1@llnl.gov

[1] B. C. Masters, Philos. Mag. **11**, 881 (1965).
[2] B. L. Eyre and A. F. Bartlett, Philos. Mag. **11**, 261 (1965).
[3] B. L. Eyre and A. F. Bartlett, J. Nucl. Mater. **47**, 143 (1973).
[4] T. J. Bullough and B. L. Eyre, Proc. R. Soc. London A **435**, 85 (1991).
[5] H. Kawanishi and E. Kuramoto, J. Nucl. Mater. **141–143**, 899 (1986).
[6] L. L. Horton and K. Farrell, J. Nucl. Mater. **122–123**, 687 (1984).
[7] B. L. Eyre and R. Bullough, Philos. Mag. **12**, 31 (1965).
[8] R. A. Johnson, Phys. Rev. **134**, 1329 (1964).
[9] B. D. Wirth, G. R. Odette, D. Maroudas, and G. E. Lucas, J. Nucl. Mater. **276**, 33 (2000).
[10] Y. N. Osetsky, A. Serra, B. N. Singh, and S. I. Golubov, Philos. Mag. A **80**, 2131 (2000).
[11] R. E. Stoller, J. Nucl. Mater. **233–237B**, 999–1003 (1996).
[12] N. Soneda and T. Diaz de la Rubia, Philos. Mag. A **78**, 995 (1998).
[13] T. Diaz de la Rubia and M. W. Guinan, Mater. Res. Forum **174**, 151 (1990).
[14] G. J. Ackland, D. J. Bacon, A. F. Calder, and T. Harry, Philos. Mag. A **75**, 713 (1997).
[15] J. P. Hirth and J. Lothe, *Theory of Dislocations* (Krieger Publishing Co., Malabar, FL, 1982), 2nd ed.
[16] J. O. Schiffgens and K. E. Garrison, J. Appl. Phys. **43**, 3240 (1972).
[17] W. Carrington, K. F. Hale, and D. McLean, Proc. R. Soc. London A **259**, 203 (1960).
[18] S. M. Ohr and D. N. Beshers, Philos. Mag. **8**, 1343 (1963).
[19] Y. N. Osetsky, A. Serra, and V. Priego, J. Nucl. Mater. **276**, 202 (2000).